

## High-pressure Raman spectroscopy of $\text{ZrSiO}_4$ : Observation of the zircon to scheelite transition at 300 K

ELISE KNITTLE, QUENTIN WILLIAMS

Department of Earth Sciences and Institute of Tectonics, University of California, Santa Cruz, California 95064, U.S.A.

### ABSTRACT

Raman spectra of  $\text{ZrSiO}_4$  to pressures of 37 GPa are presented. At  $23 \pm 1$  GPa and 300 K,  $\text{ZrSiO}_4$  undergoes a first-order phase transition from the zircon to the scheelite structure. The phase transformation is irreversible at 300 K, and  $\text{ZrSiO}_4$  (scheelite structure) is quenchable to ambient pressure. X-ray diffraction analysis of  $\text{ZrSiO}_4$  (scheelite structure) yields lattice parameters of  $a = 0.4726(12)$  nm and  $c = 1.0515(44)$  nm, in excellent agreement with those of  $\text{ZrSiO}_4$  (scheelite structure) formed under simultaneous high-pressure and high-temperature conditions. Our results support the martensitic-type mechanism for the transition from zircon structure to scheelite structure proposed to explain the shock-induced phase transformation in  $\text{ZrSiO}_4$ . Apparently, zircon is one of the few examples of a silicate that undergoes a first-order crystalline phase transformation at room temperature under compression. Because of the close structural relationship between the zircon and scheelite structures, this crystalline phase transition is likely to proceed by low-energy diffusional pathways, such as those that have been proposed to generate amorphization in some silicates when compressed metastably at 300 K.

### INTRODUCTION

Zircon,  $\text{ZrSiO}_4$ , is known to undergo a phase transition at high pressures and temperatures from shock-wave measurements (Mashimo et al., 1983; Kusaba et al., 1985, 1986) and from high-temperature investigations in a Bridgman-anvil apparatus (Reid and Ringwood, 1969) and in the laser-heated diamond cell (Liu, 1979). The high-pressure phase found from shock-recovery experiments (Kusaba et al., 1985) and the quenched products of the static, high-pressure experiments (Reid and Ringwood, 1969; Liu, 1979) are scheelite-structured (space group =  $I4_1/a$ ): this structure is closely related to the zircon structure (space group =  $I4_1/amd$ ) but is about 10% denser. In both the zircon and scheelite structures, the  $(\text{SiO}_4)^{4-}$  tetrahedral units are maintained and the  $\text{Zr}^{4+}$  is octahedrally coordinated; both structures are tetragonal. However, the  $c/a$  ratio of zircon is 0.906, whereas for  $\text{ZrSiO}_4$  (scheelite structure) it is 2.224. One of the most interesting aspects of the zircon-scheelite phase transition is that it proceeds at the microsecond time scales of shock-wave experiments, as well as under static high-pressure and temperature conditions. Indeed, the phase transition has been proposed to occur by a martensitic-type mechanism (Kusaba et al., 1986) which probably explains its occurrence under a wide variety of pressure-temperature-time conditions.

This transition is not unique to  $\text{ZrSiO}_4$ ; many other  $\text{ABO}_4$  compounds ( $A = \text{Sc}, \text{Y}$ , and the rare-earth elements;  $B = \text{As}, \text{V}$ ) that crystallize in the zircon structure are known to undergo transitions to the scheelite structure at high pressures and temperatures (Stubican and

Roy, 1963a, 1963b). For example, several Raman spectroscopic studies of rare-earth vanadates have been carried out in the diamond cell that show that the zircon to scheelite transition occurs even at 300 K in  $\text{YVO}_4$ ,  $\text{TbVO}_4$ , and  $\text{DyVO}_4$  and that the scheelite structure is quenchable to ambient pressure (Duclos et al., 1989; Jayaraman et al., 1987).

In this study, we have compressed  $\text{ZrSiO}_4$  (zircon structure) in a diamond-anvil cell at 300 K and measured Raman spectra as a function of pressure. Our goal is to determine the stability of this mineral at room temperature, to characterize its spectra at high pressures, and to investigate whether it transforms to the scheelite phase at high pressure and 300 K. Because of kinetic effects, few silicates undergo first-order crystal to crystal phase transitions at ambient temperature under simple compression. Thus, conversion of zircon to scheelite at ambient temperature implies an anomalous and possibly unique silicate transformation mechanism.

### EXPERIMENTAL

The  $\text{ZrSiO}_4$  samples used in this study are from a sand of unknown origin and are transparent single crystals 50–200  $\mu\text{m}$  in diameter. The lattice parameters of the starting material were measured by X-ray diffraction and are  $a = 0.6600(5)$  nm and  $c = 0.5978(11)$  nm, in good agreement with previous measurements (JCPDS Card no. 6-266). One single crystal of zircon was loaded into a gasketed Mao-Bell type diamond cell with a 16:3:1 mixture of methanol, ethanol, and  $\text{H}_2\text{O}$  as a pressure medium. Several small ruby grains ( $\sim 5 \mu\text{m}$  in diameter) were included

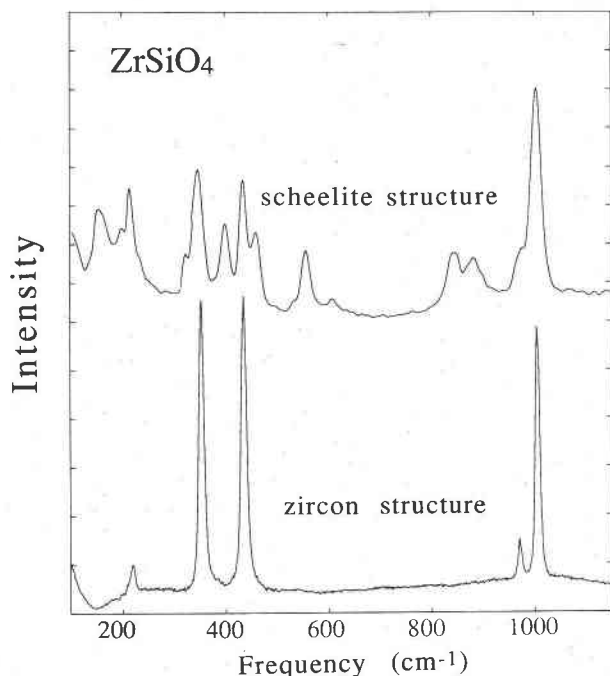


Fig. 1. Ambient-pressure Raman spectra for the ZrSiO<sub>4</sub> (zircon structure) starting material and for a sample quenched from 36.7 GPa and 300 K, which has converted to the scheelite phase. Lists of the ambient-pressure frequencies for the two spectra are given in Tables 1 and 2.

in the sample chamber, and the pressure was determined using the standard ruby fluorescence technique (Mao et al., 1978). A Coherent Innova 70-4 laser tuned to 488 nm (plasma lines were removed using an Optometrics laser monochromator) was focused into the diamond cell through an Olympus microscope using a Leitz UM-20 objective. The laser power at the sample was approximately 150–200 mW. Raman spectra from the zircon were obtained in  $\sim 360^\circ$  scattering geometry: the scattered light was focused with an Olympus zoom camera lens into the front of a Spex Triplemate spectrograph with a 1200-gr/mm holographic grating in the spectrograph stage. The spectra were recorded with an ITT model F4146 imaging microchannel plate detector coupled with a Surface Sciences Laboratory position computer and are reported with a resolution of 4 cm<sup>-1</sup>.

Raman spectra were measured on four high-pressure samples on both compression and decompression. Below 15 GPa, the pressure medium is liquid and the samples are hydrostatic, whereas above this pressure, the medium solidifies, and the pressures in the sample chamber become quasi-hydrostatic (Fujishiro et al., 1982). Therefore, the pressures for the Raman spectra measured below 15 GPa are accurate to within the error of the ruby fluorescence calibration. Above 15 GPa, Raman spectra were measured as close to a ruby chip as possible (within 10–20  $\mu\text{m}$ ) to ensure good correlation between the measured pressure and the Raman spectrum. In these samples, the

TABLE 1. ZrSiO<sub>4</sub> (zircon structure)

$\nu_0$ (cm <sup>-1</sup> )*	$d\nu/dP$ (cm <sup>-1</sup> )/ GPa)**	$\gamma$ †	Assignment‡
1006	4.8 ± 0.2	1.1 ± 0.1	$\nu_3$ : SiO <sub>4</sub> antisymmetric stretch
972	4.1 ± 0.2	1.0 ± 0.1	$\nu_1$ : SiO <sub>4</sub> symmetric stretch
436	1.1 ± 0.1	0.57 ± 0.05	$\nu_2$ : SiO <sub>4</sub> bend
355	3.2 ± 0.3	2.1 ± 0.3	lattice mode
335§	1.0 ± 0.3	0.7 ± 0.3	lattice mode?
224	—	—	lattice mode

\* All spectra are reported with a resolution of 4 cm<sup>-1</sup>.

\*\* The data fits are for all the points below the phase transition pressure (23.8 GPa).

† See text for a description of the calculation.

‡ Assignments from Syme et al. (1977) and Dawson et al. (1971).

§ Extrapolated from high pressure: this peak is observed only above 13 GPa in zircon.

error on pressure for an individual Raman spectra was estimated from the width of the ruby  $R_1$  fluorescence peak.

In addition to the high-pressure data, ambient-pressure Raman spectra and X-ray diffraction patterns were obtained from samples quenched from  $29 \pm 4$  and  $37 \pm 4$  GPa. The X-ray patterns were obtained for the individual diamond-cell samples using a Debye-Scherrer camera 114.6 mm in diameter and CuK $\alpha$  radiation.

One high-pressure and high-temperature experiment was performed to provide a comparison with the samples quenched from high pressure and 300 K to ensure that the transition to the high-pressure phase was complete. In this experiment, a sample of zircon was compressed to  $29 \pm 3$  GPa in the diamond cell and then heated (sub-solidus) with a Nd:YAG laser with a power of 25 W. This sample was decompressed, and a Raman spectrum and an X-ray pattern were obtained from the quenched sample.

## RESULTS AND DISCUSSION

### High-pressure Raman spectra of ZrSiO<sub>4</sub> (zircon structure)

At ambient pressure, we observed five peaks in the Raman spectrum of ZrSiO<sub>4</sub> (Fig. 1) in excellent agreement with previous measurements (Dawson et al., 1971; Nicola and Rutt, 1974; Syme et al., 1977). Table 1 gives the ambient-pressure frequencies with their mode assignments: the three highest frequency modes are internal stretching and bending vibrations of the (SiO<sub>4</sub>)<sup>4-</sup> tetrahedra, whereas the modes at 355 and 224 cm<sup>-1</sup> are lattice modes. We measured the pressure shifts of the four strongest modes, as illustrated in Figure 2 and quantified in Table 1. All the measured pressure shifts are positive. We note that the highest frequency mode, the (SiO<sub>4</sub>)<sup>4-</sup> antisymmetric stretching vibration, has one of the highest frequencies observed for this type of vibration in any orthosilicate, a phenomenon likely to be related to the effect of the relatively strong Zr<sup>4+</sup>-O bonds in zircon on this stretching vibration. Also, we note that the silicate

tetrahedra in zircon are among the most distorted of any silicate at ambient conditions, with a mean tetrahedral quadratic elongation of 1.02 and intratetrahedral O-Si-O angles of 97 and 116° (Robinson et al., 1971a, 1971b).

At 15 GPa, the weak symmetric stretching vibration of the (SiO<sub>4</sub>)<sup>4-</sup> tetrahedron becomes unresolvable. We attribute this to the loss of hydrostaticity in the sample above 15 GPa (the freezing point of the pressure medium), which causes broadening of this peak to the point where it is unmeasurable. An additional aspect of the high-pressure zircon spectra is the appearance at 11 GPa of a mode at slightly lower frequency than the  $\nu_4$  bending vibration and the subsequent disappearance of the  $\nu_4$  vibration, again at about 15 GPa. There are several possible explanations for this behavior. One possibility is that this is a low-frequency vibration with a large pressure shift that has shifted into the range of our high-pressure Raman measurements. However, the small change in frequency of this vibration at higher pressure indicates that this explanation is not plausible. Alternatively, the  $\nu_4$  vibration, which has E<sub>g</sub> symmetry at ambient pressure, may split because of a distortion of the crystal structure at high pressures. The appearance of the new band corresponds to a reduction in the amplitude of the  $\nu_4$  vibration, which then becomes undetectable by 15 GPa. A similar splitting of a low-frequency mode of E<sub>g</sub> symmetry is observed in the high-pressure spectrum of zircon-structured YVO<sub>4</sub> (Jayaraman et al., 1987). However, in the case of YVO<sub>4</sub>, the E<sub>g</sub> mode is thought to be accidentally degenerate, with a mode of B<sub>2g</sub> symmetry (Elliott et al., 1972); these bands have different pressure shifts and hence appear to split at high pressures. This is probably not the case with ZrSiO<sub>4</sub>, as the two analogous vibrations in this phase are separated by ~100 cm<sup>-1</sup> (Syme et al., 1977). A linear fit of our data on pressure vs. frequency for this new mode predicts a  $\nu_0$  value of 335 cm<sup>-1</sup>, only about 20 cm<sup>-1</sup> lower than the  $\nu_4$  mode; therefore, we believe the most plausible explanation for the appearance of this band is that the double degeneracy of the original  $\nu_4$  (E<sub>g</sub>) vibration has been removed through crystallographic distortion.

Table 1 also includes calculated mode Grüneisen parameters ( $\gamma_i$ ) for zircon. Because of the pressure range of our measurements, we assume that  $q$ , the logarithmic derivative of the Grüneisen parameter with volume ( $d \ln \gamma / d \ln V$ ), is near zero for these modes. Therefore,  $\gamma_i = K_T (d\nu/dP)_0 / \nu_0$  where  $\gamma_i$  is the mode Grüneisen parameter,  $K_T$  is the isothermal bulk modulus,  $\nu_0$  is the ambient-pressure frequency and  $(d\nu/dP)_0$  is the ambient pressure mode shift (Table 1). For these calculations, we use a bulk modulus of  $227 \pm 2$  GPa (Hazen and Finger, 1979). For zircon, we have measured mode Grüneisen parameters for four modes only; therefore, we do not compare our average spectroscopic Grüneisen parameter with the thermodynamic Grüneisen parameter ( $\gamma_{th} = \alpha_v K_S / \rho C_p$ ). However, previous estimates of the thermal Grüneisen parameter of zircon range from  $\gamma_{th} = 0.545$  to 1.09 (Falzone and Stacey, 1982; Özkan and Cartz, 1974; Sirdeshmukh and Subhadra, 1975; Özkan and Jamieson, 1978). The

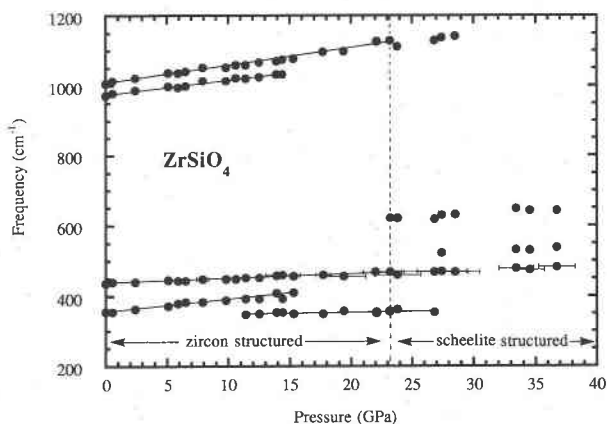


Fig. 2. Raman frequencies of ZrSiO<sub>4</sub> as a function of pressure. The errors in pressure are shown for the data with an ambient-pressure frequency of 436 cm<sup>-1</sup>. Up to pressures of 23 GPa, ZrSiO<sub>4</sub> is with the zircon structure. The appearance of a new vibrational mode at 612 cm<sup>-1</sup> at this pressure indicates that a transformation to the scheelite structure has taken place.

large difference in the reported values of  $\gamma$  is due primarily to a difference of 50% in the measured value of the volume thermal expansion coefficient between that of Falzone and Stacey (1982) and other workers (see Subbarao et al., 1990, for a summary of thermal expansion measurements on zircon). We note that the simple average of the mode Grüneisen parameters of the four measured zircon vibrational modes is 1.1. It is possible that, as in vanadates with the zircon structure, there are unmeasured lattice vibrations that exhibit soft mode behavior with pressure, thus producing a low value of  $\gamma_{th}$  (Duclos et al., 1989; Jayaraman et al., 1987).

Our vibrational mode shifts for the (SiO<sub>4</sub>)<sup>4-</sup> internal vibrations with pressure in zircon compare favorably with the mode shifts of the same vibrations in other orthosilicates, such as olivines and garnets. For example, the shift with pressure of the stretching frequencies ( $\nu_1$  and  $\nu_3$ ) in forsterite range from 1.7 to 5.2 cm<sup>-1</sup>/GPa, in fayalite from 2.5 to 3.5 cm<sup>-1</sup>/GPa, and in the garnets pyrope, grossularite, and almandine, from 3.4 to 4.7 cm<sup>-1</sup>/GPa (Hofmeister et al., 1989; Mernagh and Liu, 1990; Knittle et al., 1992). Therefore, the large pressure shifts for the tetrahedral vibrations in zircon, 4.8 and 4.1 cm<sup>-1</sup>/GPa (Table 1), are compatible with results for other silicates containing isolated tetrahedra. For pyrope and grossularite, the silicate bending modes (three total) have pressure shifts of 3.6–3.8 cm<sup>-1</sup>/GPa; and for forsterite and fayalite, the pressure shifts of the bending vibrations fall generally into two groups: those with pressure shifts of 1.0–1.5 cm<sup>-1</sup>/GPa, and those with pressure shifts of 2.7–3.2 cm<sup>-1</sup>/GPa. Thus, a small pressure shift for the (SiO<sub>4</sub>)<sup>4-</sup> bending vibration in zircon, 1.1 cm<sup>-1</sup>/GPa, is compatible with the results for olivines. However, the relatively high bulk modulus of zircon produces mode Grüneisen parameters that are about 10–20% larger than those of garnets and 20–60% larger than those of olivine for (SiO<sub>4</sub>)<sup>4-</sup>

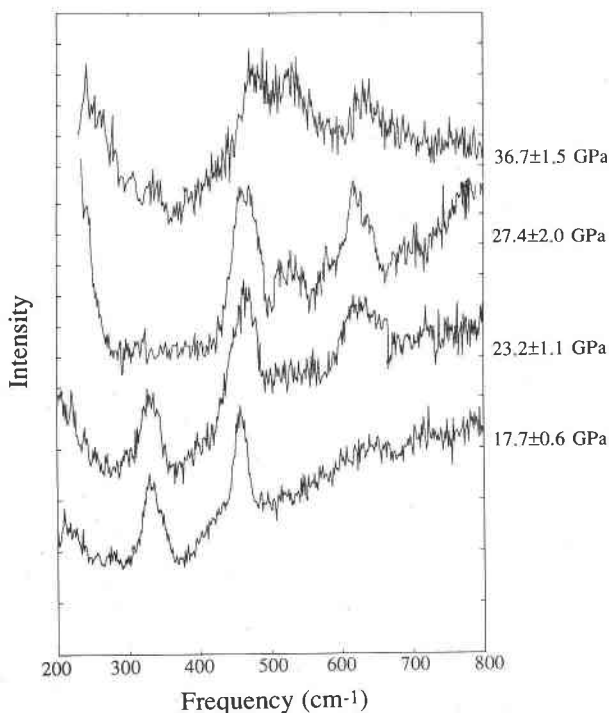


Fig. 3. Representative Raman spectra through the phase transition from zircon to scheelite structure. Spectra are presented from 200 to 800  $\text{cm}^{-1}$ , which is the diagnostic frequency region for the transformation. The bottom spectrum is at  $17.7 \pm 0.6$  GPa, within the metastability range of the phase with the zircon-structure. The spectrum at  $23.2 \pm 1.1$  GPa shows the first appearance of a vibration of the phase with the scheelite structure at  $612 \text{ cm}^{-1}$ , and the spectrum at  $27.4 \pm 2.0$  GPa shows the appearance of a second peak in the phase with the scheelite structure at  $520 \text{ cm}^{-1}$ . In addition, in the spectrum at 27.4 GPa, the lowest frequency vibration of the zircon structure has become undetectable. The top spectrum is at the highest pressure of our study,  $36.7 \pm 1.5$  GPa, and is of the phase with the scheelite structure. The strong peak that is at  $460 \text{ cm}^{-1}$  at 17.7 GPa is not the same vibration as the peak observed at  $480 \text{ cm}^{-1}$  at 36.7 GPa, because of the change in phase.

stretching bands (Hofmeister et al., 1989; Mernagh and Liu, 1990; Knittle et al., 1992). Accordingly, we infer that the amount of compression undergone by the silicate tetrahedron in zircon per unit volume of compaction is more extreme than that in other orthosilicate phases; this is consistent with single-crystal X-ray diffraction results on zircon to 4.8 GPa (Hazen and Finger, 1979).

#### Phase transformation and Raman spectra of ZrSiO<sub>4</sub> (scheelite structure)

The most obvious change in the spectrum of ZrSiO<sub>4</sub> occurs at  $23.2 \pm 1.1$  GPa, where a new band appears in the spectrum at about  $610 \text{ cm}^{-1}$ , and the frequencies of the strong  $\nu_3$  and  $\nu_2$  vibrations shift abruptly downward by 17 and  $10 \text{ cm}^{-1}$ , respectively, between 23.2 and 23.8 GPa. These changes in the spectrum are consistent with a high-pressure phase transition from the zircon structure

to the scheelite structure, as observed for other compounds with the zircon structure at 300 K (Jayaraman et al., 1987; Duclos et al., 1989). Indeed, that the scheelite structure is formed in these samples is confirmed by the X-ray diffraction results on decompressed samples described below. As pressure is increased, another new vibration appears at about  $520 \text{ cm}^{-1}$  at  $27.4 \pm 2.0$  GPa, and the lowest frequency vibration of the zircon structure, which is extremely weak above 20 GPa, becomes unresolvable. Figure 3 illustrates the changes in the low-frequency region of the Raman spectra as pressure is increased through the phase transition. In addition, the highest frequency vibration also disappears above 28.5 GPa. However, the disappearance of this band may simply reflect a high degree of distortion of the SiO<sub>4</sub> tetrahedron in the scheelite structure at these pressures, which produces a weakened and broadened band [no data are presently available on the distortion of the SiO<sub>4</sub> tetrahedra in ZrSiO<sub>4</sub> (scheelite structure); however, the tetrahedra in germanates with the scheelite structure are considerably distorted (Vandenborre et al., 1989)]. We note that at 28.5 GPa, this vibration is at  $1150 \text{ cm}^{-1}$ , by far the highest frequency ever observed for a stretching vibration of an isolated silicate tetrahedron.

The vibrational modes of the ZrSiO<sub>4</sub> (scheelite structure) are measured to nearly 37 GPa and on decompression. Figure 4 is a plot of these data, and pressure shifts of these modes are tabulated in Table 2. The low-frequency vibrations can be tracked continuously on decompression; however, the high-frequency SiO<sub>4</sub> internal modes are not resolved until pressures below 6 GPa are reached. Upon decompression, two more new modes appear in the spectra of the scheelite structure below 6 GPa, at about  $900 \text{ cm}^{-1}$  ( $\nu_0 = 880 \text{ cm}^{-1}$ ) and  $420 \text{ cm}^{-1}$  ( $\nu_0 = 392 \text{ cm}^{-1}$ ). When the sample is completely decompressed, several additional peaks are resolved, particularly at low frequency (see Fig. 1 and Table 2). Most of these peaks are weak or shoulders of stronger vibrations. However, the peaks at 880 and  $842 \text{ cm}^{-1}$  have about the same amplitude, although only that at  $880 \text{ cm}^{-1}$  is observed at high pressure. It is possible that the single mode observed at high pressure is actually two peaks, with the splitting not being resolvable until the sample is fully decompressed.

Our mode assignments for the ZrSiO<sub>4</sub> (scheelite structure) are given in Table 2. For the Raman-active modes of scheelite structures, factor group analysis predicts seven internal modes: three stretching vibrations of the (SiO<sub>4</sub>)<sup>4-</sup> tetrahedra [ $\nu_1$  ( $A_g$  symmetry),  $\nu_3$  ( $E_g$ ), and  $\nu_3$  ( $B_g$ )] and four bending vibrations [ $\nu_2$  ( $A_g$ ),  $\nu_2$  ( $B_g$ ),  $\nu_4$  ( $B_g$ ), and  $\nu_4$  ( $E_g$ )]. Additionally, six external modes are predicted: two rotations,  $A_g$  and  $E_g$ , and four translations,  $2B_g$  and  $2E_g$  (cf. Porto and Scott, 1967; Liegeois-Duyckaerts and Tarte, 1972; Vandenborre et al., 1989). It is not unusual for all thirteen predicted Raman-active vibrations to appear in scheelite-type molybdates, tungstates, and germanates (Porto and Scott, 1967; Vandenborre et al., 1989). However, we note that we observe fourteen Raman ac-

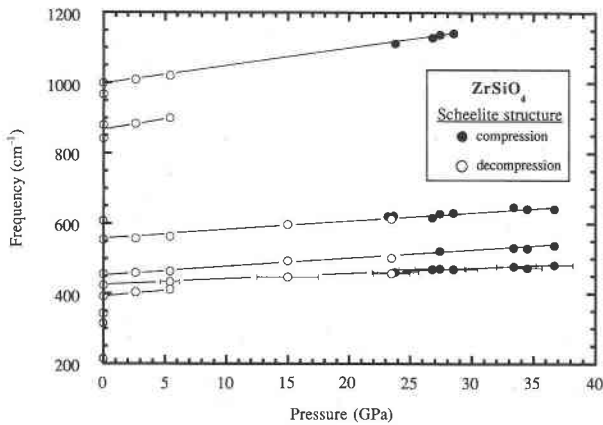


Fig. 4. Pressure shifts of the vibrational frequencies of ZrSiO<sub>4</sub> (scheelite structure). The closed circles were obtained on compression of the samples, and the open circles were obtained on decompression. The error bars in pressure are shown for the data points of the mode with an ambient-pressure frequency of 424 cm<sup>-1</sup>.

tive vibrations at ambient pressure (see Fig. 1 and Table 2), probably as a result of residual strain in the decompressed samples: scheelite appears to be particularly susceptible to such strain-induced mode activity (e.g., Scott, 1968; Miller et al., 1973).

We assign the highest-frequency Raman vibration in ZrSiO<sub>4</sub> (scheelite structure) to a  $\nu_3$  antisymmetric stretch ( $B_g$  symmetry), with the weak shoulder as a  $\nu_1$  symmetric stretch ( $A_g$  symmetry). This differs from assignments for molybdates, vanadates, and tungstates with the scheelite and zircon structures; where  $\nu_1$  vibrations lie at higher frequencies than  $\nu_3$ -derived vibrations (Porto and Scott, 1967; Miller et al., 1968; Liegeois-Duyckaerts and Tarte, 1972; Jayaraman et al., 1987; Duclos et al., 1989). However, the  $\nu_3$  vibrations of silicates are generally higher in frequency than their  $\nu_1$  vibrations, and from polarized Raman studies of single crystal ZrSiO<sub>4</sub> (zircon structure), the  $\nu_3$  antisymmetric stretching vibration seems unquestionably to be at higher frequency than the  $\nu_1$  symmetric stretching vibration (Dawson et al., 1971; Syme et al., 1977). Thus, by analogy with ZrSiO<sub>4</sub> (zircon structure) and because of the similarity of assignments between the highest frequency bands in isochemical vanadates with zircon structure and scheelite structure, we assign the highest lying peaks in ZrSiO<sub>4</sub> (scheelite structure) to  $\nu_3$  vibrations. We note that in a study of germanates with scheelite structure (including ZrGeO<sub>4</sub>), Vandenberg et al. (1989) assign the highest frequency vibration to a  $\nu_1$ -derived mode based on a normal coordinate analysis; however, we believe that for ZrGeO<sub>4</sub>, the highest frequency mode is  $\nu_3$ -derived rather than  $\nu_1$ -derived.

The assignments of the modes at 880 and 842 cm<sup>-1</sup> are uncertain: germanates with the scheelite structure have only one vibration in their analogous spectral region (Vandenberg et al., 1989). Therefore, the higher frequency vibration at 880 cm<sup>-1</sup> is probably the second  $\nu_3$ -

TABLE 2. ZrSiO<sub>4</sub> (scheelite structure)

$\nu_0$ (cm <sup>-1</sup> ) <sup>*</sup>	$d\nu/dP$ (cm <sup>-1</sup> /GPa) <sup>**</sup>	Assignment <sup>†</sup>
1001 (s)	5.0 ± 0.1	$\nu_3$ : SiO <sub>4</sub> antisymmetric stretch
967‡ (sh)	—	$\nu_1$ : SiO <sub>4</sub> symmetric stretch
880 (m)	3.7 ± 1.2	$\nu_3$ : SiO <sub>4</sub> antisymmetric stretch
842‡ (m)	—	strain-activated mode?
604‡ (w)	—	$\nu_4$ : SiO <sub>4</sub> bend
552 (m)	2.6 ± 0.1	$\nu_4$ : SiO <sub>4</sub> bend
456 (m)	2.2 ± 0.1	$\nu_2$ : SiO <sub>4</sub> bend
424 (m)	1.5 ± 0.1	$\nu_2$ : SiO <sub>4</sub> bend
392 (m)	3.7 ± 0.5	lattice mode
343‡ (m)	—	lattice mode
320‡ (sh)	—	lattice mode
216‡ (m)	—	lattice mode
196‡ (sh)	—	lattice mode
154‡ (m)	—	lattice mode

\* Relative peak heights estimated visually: s = strong, m = medium, w = weak, sh = shoulder.

\*\* The fit is to points taken on compression at and above 23.8 GPa and those on decompression.

† See text for a more complete description.

‡ Not observed at high pressure.

derived antisymmetric stretch ( $E_g$  symmetry). It is possible that the other band at 842 cm<sup>-1</sup> is a strain-induced mode. Such strain-induced mode activation has been observed for CaWO<sub>4</sub> and CaMoO<sub>4</sub> with the scheelite structure where high-frequency inactive modes become activated by shear strain (Scott, 1968).

The four Raman-active vibrations at 604, 552, 456, and 424 cm<sup>-1</sup> are probably bending modes of the SiO<sub>4</sub> tetrahedra; however, which of these are predominately associated with  $\nu_2$  vibrations and which with  $\nu_4$  vibrations is uncertain. Previous assignments of the bending vibrations for scheelite-structured compounds have placed the  $\nu_4$  vibrations at higher frequency than the  $\nu_2$  vibrations (Porto and Scott, 1967; Liegeois-Duyckaerts and Tarte, 1972; Miller et al., 1973; Jayaraman et al., 1987; Duclos et al., 1989; Vandenberg et al., 1989). Additionally, in ZrSiO<sub>4</sub> (zircon structure),  $\nu_4$  vibrations are at higher frequency than  $\nu_2$  (Syme et al., 1977; note that this assignment differs from that of Dawson et al., 1971). Given the similarities between the zircon and scheelite structures of ZrSiO<sub>4</sub>, we tentatively assign the two higher frequency peaks as  $\nu_4$  vibrations. The remaining six vibrational bands are all external modes, in accord with the assignments of Porto and Scott (1967) and Vandenberg et al. (1989).

### X-ray diffraction results

To investigate the structure of the quenched phase of ZrSiO<sub>4</sub>, we measured the Raman spectrum and X-ray diffraction patterns of samples quenched from 28 ± 4 GPa and 300 K (a pressure about 4 GPa above the appearance of the new Raman peaks), 37 ± 4 GPa and 300 K (the highest pressure of our study), and 29 ± 3 GPa, following laser-heating to ~1800 K. For the samples quenched from 37 GPa and 300 K and from 29 GPa and 1800 K, the X-ray diffraction patterns contained lines of only ZrSiO<sub>4</sub> (scheelite structure) (Table 3 lists the ob-

TABLE 3. X-ray diffraction pattern of ZrSiO<sub>4</sub> (scheelite structure)

<i>d</i> value (Å)	<i>hkl</i>
4.339 ± 0.008	101
2.824 ± 0.005	112
2.625 ± 0.004	004
2.377 ± 0.004	200
2.082 ± 0.003	211
1.906 ± 0.003	105
1.814 ± 0.002	213
1.763 ± 0.003	204
1.653 ± 0.003	220
1.555 ± 0.002	116
1.442 ± 0.002	312

served *d* values and *hkl* assignments). The X-ray diffraction lines were relatively broad, an observation also noted and analyzed for shock-generated ZrSiO<sub>4</sub> by Kusaba et al. (1986), who concluded that this line broadening in ZrSiO<sub>4</sub> (scheelite structure) was indicative of a high degree of residual strain. The ZrSiO<sub>4</sub> with the scheelite structure has lattice parameters of *a* = 0.4726(12) nm and *c* = 1.0515(44) nm, in accord with those measured in previous experiments, as given in Table 4 (Reid and Ringwood, 1969; Liu, 1979; Kusaba et al., 1985). In addition, the ambient-pressure Raman spectrum of the laser-heated sample is identical to that of the sample quenched from 300 K, with the exception that one additional weak vibration is seen at 651 cm<sup>-1</sup> in the laser-heated sample.

The X-ray pattern of the sample quenched from 28 GPa and 300 K had diffraction lines of both ZrSiO<sub>4</sub> with the zircon structure and ZrSiO<sub>4</sub> with the scheelite structure. However, micro-Raman spectroscopy of the quenched sample showed that the central regions of the sample, which had been at the highest pressure, had the Raman spectrum of only the ZrSiO<sub>4</sub> (scheelite structure). The extreme edges of the sample (nearest the gasket) had the Raman spectrum of only zircon. Therefore, both phases existed in this quenched sample, but not in the same regions.

We did not observe the further breakdown of the scheelite structure under laser-heating to ZrO<sub>2</sub> (cotunnite structure) plus SiO<sub>2</sub> (stishovite), as reported by Liu (1979). From both our X-ray diffraction and Raman spectroscopy on the sample quenched from 29 GPa and ~1800 K, the ZrSiO<sub>4</sub> remains in the scheelite structure under these conditions. We suggest that either Liu's samples were at higher pressures than the 20–25 GPa estimated from spring-length calibrations or that differences in sample temperature between our study and his could control the phases present in the two studies.

#### Mechanism and kinetics of the phase transformation

There are two particularly notable aspects of the phase transformation from zircon to scheelite in ZrSiO<sub>4</sub>. First, its occurrence at 300 K is unusual among silicates. To our knowledge, no other silicate undergoes a first-order, crystal to crystal phase transformation with such a large volume change (~10%) by simple compression at 300 K;

TABLE 4. Lattice parameters of ZrSiO<sub>4</sub> (scheelite structure)

<i>a</i> (nm)	<i>c</i> (nm)	Reference
0.4726(12)	1.0515(44)	this study
0.4730	1.0480	Reid and Ringwood, 1969
0.4712(2)	1.0450(10)	Liu, 1979
0.4734(1)	1.0511(1)	Kusaba et al., 1985

such phase transitions in other silicates typically proceed only at temperatures greater than about 900 K (Liu and Bassett, 1986). Second, the irreversibility of the transition from zircon structure to scheelite structure is extreme: not only is the scheelite structure quenchable in pressure at 300 K, but at ambient pressure, temperatures of greater than ~1273 K are required to return the scheelite structure to the zircon structure (Kusaba et al., 1985). The kinetics of this transformation are consistent with the two-step model proposed by Kusaba et al. (1986), in which the [110] direction of zircon is converted to the [001] direction of scheelite by a simple shearing mechanism. The second step (which may occur simultaneously with the shearing) incorporates small displacements of atoms, including rotations of SiO<sub>4</sub>-tetrahedra. In both steps, the SiO<sub>4</sub> tetrahedral units are maintained with neither Si<sup>4+</sup> nor Zr<sup>4+</sup> undergoing a change in coordination.

However, whereas the mechanism of Kusaba et al. (1986) readily explains the rapidity of the zircon to scheelite transition under shock loading, it does not dictate whether (or the degree to which) this transition is thermally activated. Calculated Hugoniot temperatures of zircon vary from ~600 to 1200 K between 30 and 50 GPa, the pressure range over which the yield of ZrSiO<sub>4</sub> (scheelite structure) increases in shock-loaded samples (Mashimo et al., 1983; Kusaba et al., 1985). However, localized hot spots whose temperatures exceed calculated Hugoniot temperatures are well known in shock-loaded samples (e.g., Schmitt and Ahrens, 1989). Thus, these results provide little constraint on the role of temperature in driving this transition.

It is notable that the actual equilibrium transition pressure from zircon to scheelite at 300 K is probably less than ~12 GPa, the pressure at which this transition has been documented to occur in high-temperature static experiments (Reid and Ringwood, 1969; Liu, 1979); we assume that this transformation has a positive Clapeyron slope, as do other zircon to scheelite transitions (Stubican and Roy, 1963a, 1963b). Thus, our observation that this transition does not occur until near 23 GPa at 300 K indicates that even the minor diffusional motion necessary within the model of Kusaba et al. (1986) causes the transformation to be kinetically impeded. That this transition ultimately occurs at 300 K after considerable overdriving in pressure implies that the activation energy for the transformation has decreased with compression to the degree that the transition can occur at this markedly low temperature (for silicates). In short, it appears that the diffusional motion necessary to conduct the zircon to scheelite transformation is associated with a sufficiently

low-energy pathway at 23 GPa that the transformation can proceed even at 300 K. Finally, because we observe the transition to occur at identical pressures in different samples (with different pressure gradients), we do not believe shear stress plays a major role in determining the pressure of this transition at 300 K.

It is notable that such low-energy diffusional pathways have been proposed to produce the transition at 300 K and 20–30 GPa of quartz to an amorphous form (Binggeli and Chelikowsky, 1991). Such amorphization has been documented for a wide range of metastably compressed silicates at 300 K, varying from silicates with olivine structure to feldspars and silica polymorphs (Williams et al., 1990; Williams and Jeanloz, 1989; Hemley, 1987). We view it as likely that low-energy diffusional paths are required to produce first-order transformations in compressed silicates at 300 K, and we speculate that although such paths may lead to amorphization in some metastably compressed silicates, the zircon structure is unique in having a low-energy means by which it can transform to a closely related (and considerably denser) crystal structure when compressed metastably.

#### ACKNOWLEDGMENTS

This work is supported by the W.M. Keck Foundation and the NSF. We thank R. Hemley and S. Sharma for helpful comments on the manuscript. Institute of Tectonics Contribution no. 173 (Mineral Physics Lab).

#### REFERENCES CITED

- Binggeli, N., and Chelikowsky, J.R. (1991) Structural transformation of quartz at high pressures. *Nature*, 335, 344–346.
- Dawson, P., Hargreave, M.M., and Wilkinson, G.R. (1971) The vibrational spectrum of zircon (ZrSiO<sub>4</sub>). *Journal of Physics C: Solid State Physics*, 4, 240–256.
- Duclos, S.J., Jayaraman, A., Espinosa, G.P., Cooper, A.S., and Maines, R.G. (1989) Raman and optical absorption studies of the pressure-induced zircon to scheelite structure transformation in TbVO<sub>4</sub> and DyVO<sub>4</sub>. *Journal of Physics and Chemistry of Solids*, 50, 769–775.
- Elliott, R.J., Harley, R.T., Hayes, W., and Smith, S.R.P. (1972) Raman scattering and theoretical studies of the John-Teller induced phase transitions in some rare-earth compounds. *Proceedings of the Royal Society of London, Series A*, 328, 217–266.
- Falzone, A.J., and Stacey, F.D. (1982) Measurements of thermal expansions of small mineral crystals. *Physics and Chemistry of Minerals*, 8, 212–217.
- Fujishiro, I., Piermarini, G.J., Block, S., and Munro, R.G. (1982) Viscosity and glass transition pressures in the methanol-ethanol-water system. In C.M. Backman, T. Johannsson, and L. Tegner, Eds., *High pressure research in science and industry*, p. 608–611. Arkitektkopia, Uppsala, Sweden.
- Hazen, R.M., and Finger, L.W. (1979) Crystal structure and compressibility of zircon at high pressure. *American Mineralogist*, 64, 196–201.
- Hemley, R.J. (1987) Pressure dependence of the Raman spectra of SiO<sub>2</sub> polymorphs:  $\alpha$ -quartz, coesite and stishovite. In M.H. Manghni and Y. Syono, Eds., *High pressure research in mineral physics*, p. 347–360. Terra Scientific, Tokyo.
- Hofmeister, A.M., Xu, J., Mao, H.K., Bell, P.M., and Hoering, T.C. (1989) Thermodynamics of Fe-Mg olivines at mantle pressures: Mid- and far-infrared spectroscopy at high pressure. *American Mineralogist*, 74, 281–306.
- Jayaraman, A., Kourouklis, G.A., Espinosa, G.P., Cooper, A.S., and VanUitert, L.G. (1987) A high-pressure Raman study of yttrium vanadate (YVO<sub>4</sub>) and the pressure-induced transition from the zircon-type to the scheelite-type structure. *Journal of Physics and Chemistry of Solids*, 50, 755–759.
- Knittle, E., Hathorne, A., Davis, M., and Williams, Q. (1992) A spectroscopic study of the high-pressure behavior of the O<sub>4</sub>H<sub>4</sub> substitution in garnet. In M.H. Manghni and Y. Syono, Eds., *High pressure research in mineral physics*, p. 297–304. Terra Scientific, Tokyo.
- Kusaba, K., Syono, Y., Kikuchi, M., and Fukuoka, K. (1985) Shock behavior of zircon: Phase transition to scheelite structure and decomposition. *Earth and Planetary Science Letters*, 72, 433–439.
- Kusaba, K., Yagi, T., Kikuchi, M., and Syono, Y. (1986) Structural considerations on the mechanism of the shock-induced zircon-scheelite transition in ZrSiO<sub>4</sub>. *Journal of Physics and Chemistry of Solids*, 47, 675–679.
- Liegeois-Duyckaerts, M., and Tarte, P. (1972) Vibrational studies of molybdates, tungstates and related compounds. II. New Raman data and assignments for the scheelite-type compounds. *Spectrochimica Acta*, 28A, 2037–2051.
- Liu, L.G. (1979) High-pressure phase transformations in baddeleyite and zircon, with geophysical implications. *Earth and Planetary Science Letters*, 44, 390–396.
- Liu, L.G., and Bassett, W.A. (1986) *Elements, oxides, and silicates*, 250 p. Oxford University Press, New York.
- Mao, H.K., Bell, P.M., Shaner, J.W., and Steinberg, D.J. (1978) Specific volume measurements of Cu, Mo, Pd and Ag and calibration of the ruby R<sub>1</sub> fluorescence pressure gauge from 0.06 to 1 Mbar. *Journal of Applied Physics*, 49, 3276–3283.
- Mashimo, T., Nagayama, K., and Sawaoka, A. (1983) Shock compression of zirconia ZrO<sub>2</sub> and zircon ZrSiO<sub>4</sub> in the pressure range up to 150 GPa. *Physics and Chemistry of Minerals*, 9, 237–247.
- Mernagh, T.P., and Liu, L.G. (1990) Pressure dependence of Raman spectra from the garnet end-members pyrope, grossularite and almandite. *Journal of Raman Spectroscopy*, 21, 305–309.
- Miller, P.J., Khanna, R.K., and Lippincott, E.R. (1973) Studies of coupled molybdate and tungstate vibrations. *Journal of Physics and Chemistry of Solids*, 34, 533–540.
- Miller, S.A., Caspers, H.H., and Rast, H.E. (1968) Lattice vibrations of yttrium vanadate. *Physical Review*, 168, 964–969.
- Nicola, J.H., and Rutt, H.N. (1974) A comparative study of zircon (ZrSiO<sub>4</sub>) and hafnon (HfSiO<sub>4</sub>) Raman spectra. *Journal of Physics C: Solid State Physics*, 7, 1381–1386.
- Özkan, H., and Cartz, L. (1974) Anisotropic thermophysical properties of zircon. In R.E. Taylor and G.L. Denman, Eds., *A.I.P. Conference Proceedings, Thermal Expansion*, p. 21–33. American Institute of Physics, New York.
- Özkan, H., and Jamieson, J.C. (1978) Pressure dependence of the elastic constants of nonmetamict zircon. *Physics and Chemistry of Minerals*, 2, 215–224.
- Porto, S.P.S., and Scott, J.F. (1967) Raman spectra of CaWO<sub>4</sub>, SrWO<sub>4</sub>, CaMoO<sub>4</sub> and SrMoO<sub>4</sub>. *Physical Review*, 157, 716–719.
- Reid, A.F., and Ringwood, A.E. (1969) Newly observed high pressure transformations in Mn<sub>2</sub>O<sub>4</sub>, CaAl<sub>2</sub>O<sub>4</sub> and ZrSiO<sub>4</sub>. *Earth and Planetary Science Letters*, 6, 205–208.
- Robinson, K., Gibbs, G.V., and Ribbe, P.H. (1971a) Quadratic elongation: A quantitative measure of distortion in coordination polyhedra. *Science*, 172, 568–570.
- (1971b) The structure of zircon: A comparison with garnet. *American Mineralogist*, 56, 782–791.
- Schmitt, D.R., and Ahrens, T.J. (1989) Shock temperatures in silica glass: Implications for modes of shock-induced deformation, phase transformation, and melting with pressure. *Journal of Geophysical Research*, 94, 5851–5871.
- Scott, J.F. (1968) Lattice perturbations in CaWO<sub>4</sub> and CaMoO<sub>4</sub>. *Journal of Chemical Physics*, 48, 874–876.
- Sirdeshmukh, S., and Subhadra, K.G. (1975) Note on the elastic properties of zircon. *Journal of Applied Physics*, 46, 3681–3682.
- Stubican, V.S., and Roy, R. (1963a) Relation of equilibrium phase-transition pressure to ionic radii. *Journal of Applied Physics*, 34, 1888–1890.
- (1963b) High-pressure scheelite structure polymorphs of rare-earth vanadates and arsenates. *Zeitschrift für Kristallographie*, 119, 90.
- Subbarao, E.C., Agrawal, D.K., McKinstry, H.A., SALLESE, C.W., and Roy, R. (1990) Thermal expansion of compounds of zircon structure. *Journal of the American Ceramic Society*, 73, 1246–1252.

- Syme, R.W.G., Lockwood, D.J., and Kerr, H.J. (1977) Raman spectrum of synthetic zircon (ZrSiO<sub>4</sub>) and thorite (ThSiO<sub>4</sub>). *Journal of Physics C: Solid State Physics*, 10, 1335–1348.
- Vandenborre, M.T., Michel, D., and Ennacir, A. (1989) Vibrational spectra and force fields of scheelite-type germanates. *Spectrochimica Acta*, 45A, 721–727.
- Williams, Q., and Jeanloz, R. (1989) Static amorphization of anorthite at 300 K and comparison with diaplectic glass. *Nature*, 338, 413–415.
- Williams, Q., Knittle, E., Reichlin, R., Martin, S., and Jeanloz, R. (1990) Structural and electronic properties of Fe<sub>2</sub>SiO<sub>4</sub>-fayalite at ultrahigh pressures: Amorphization and gap closure. *Journal of Geophysical Research*, 95, 21549–21563.

MANUSCRIPT RECEIVED MAY 26, 1992

MANUSCRIPT ACCEPTED NOVEMBER 24, 1992